

## Magnetic polaron and Fermi surface effects in the spin-flip scattering of $\text{EuB}_6$

R. R. Urbano,<sup>1</sup> P. G. Pagliuso,<sup>1</sup> C. Rettori,<sup>1</sup> S. B. Oseroff,<sup>2</sup> J. L. Sarrao,<sup>3</sup> P. Schlottmann,<sup>4</sup> and Z. Fisk<sup>4</sup>

<sup>1</sup>*Instituto de Física "Gleb Wataghin," UNICAMP, 13083-970, Campinas-São Paulo, Brazil*

<sup>2</sup>*San Diego State University, San Diego, California 92182, USA*

<sup>3</sup>*Los Alamos National Laboratory, Los Alamos, New Mexico 87545, USA*

<sup>4</sup>*National High Magnetic Field Laboratory, Florida State University, Tallahassee, Florida 32310, USA*

(Received 28 April 2004; published 5 October 2004)

The spin-flip scattering (SFS) between conduction and  $4f^7 \text{Eu}^{2+} (^8S_{7/2})$  electrons in the paramagnetic phase of  $\text{EuB}_6$  ( $T \geq 2T_c \approx 30$  K) is studied by means of electron spin resonance (ESR) at three frequencies. The single Dysonian resonance observed in all cases suggests a *metallic* environment for the  $\text{Eu}^{2+}$  ions. The ESR at high field,  $H \approx 12.05$  kG ( $\nu \approx 33.9$  GHz), has an anisotropic linewidth with cubic symmetry. The low-field, 1.46 kG (4.1 GHz) and 3.35 kG (9.5 GHz), ESR linewidths are unexpectedly broader and have a smaller anisotropy than at the higher field. The unconventional narrowing and anisotropy of the linewidth at higher fields are indicative of a homogeneous resonance and microscopic evidence for a strong reduction in spin-flip scattering between the spins of  $\text{Eu}^{2+}$  and the states in the *electron* and *hole* pockets at the  $X$  points of the Brillouin zone by magnetic polarons.

DOI: 10.1103/PhysRevB.70.140401

PACS number(s): 75.10.Lp, 71.10.Ca, 71.35.-y

$\text{EuB}_6$  crystallizes in a simple cubic lattice with the  $\text{B}_6$ -octahedra at the corners and the  $\text{Eu}^{2+}$  ions ( $^8S_{7/2}$  Hund's rule ground state) at the body center of the unit cells. At high temperatures ( $T$ ),  $\text{EuB}_6$  is a low carrier density semimetal that is intrinsically uncompensated (more electrons than holes).<sup>1-4</sup> With decreasing  $T$ ,  $\text{EuB}_6$  undergoes a two-step transition from the paramagnetic (PM) to a ferromagnetic (FM) phase with  $T_{c1} \approx 15.3$  K and  $T_{c2} \approx 12.6$  K.<sup>5-7</sup> This magnetic transition is accompanied by a dramatic reduction in the resistivity and attributed to the spontaneous formation of magnetic polarons,<sup>8</sup> i.e., the spins of the carriers polarize the spins of the surrounding  $\text{Eu}^{2+}$  ions. The magnetic polarons form in the PM phase and grow in size as  $T$  is lowered and  $H$  is increased, giving rise to electronic and magnetic phase separation above  $T_{c2}$ .<sup>5-7</sup> At  $T_{c1}$  the polarons form a percolative network with the concomitant transition from semimetal to metal. Homogeneous FM is only established below  $T_{c2}$ .<sup>8,9</sup> The effective mass of the carriers decreases,<sup>7,10</sup> and the carrier concentration increases across the transitions when  $T$  is lowered.<sup>11</sup>

The microscopic mechanisms responsible for the earlier properties are, however, unclear. In particular, the exchange interaction between the  $\text{Eu}^{2+}$  and the conduction states is crucial for the low- $T$  magnetic and transport properties.<sup>12,13</sup> From band structure calculations it is known that the  $\text{Eu}^{2+}$  spins ferromagnetically couple predominantly to states in the electron pockets at the  $X$  points of the Brillouin zone.<sup>2</sup> Thus, Eu-site magnetic spectroscopy techniques such as ESR can provide very useful insight. Two previous reports on ESR in polycrystalline<sup>14</sup> and single-crystalline<sup>15</sup>  $\text{EuB}_6$  only partially described the features observed in the ESR spectra of  $\text{EuB}_6$ . Moreover, neither focused in probing details of the microscopic magnetic interaction nor on the influence of magnetic polarons on the SFS in the PM regime. The aim of the present work is to further explore ESR in  $\text{EuB}_6$  using various magnetic fields ( $H$ ) (frequencies) and as a function of  $T$ . The ESR linewidth is related to the SFS, which is then correlated to the electrical magnetoresistivity (MR).

Our main result is an unusual narrowing of the ESR peak-to-peak linewidth ( $\Delta H$ ) at high  $H$  having cubic anisotropy. The cubic anisotropy itself is a surprising result, because the Koringa relaxation is usually isotropic. A comparison with the anisotropy of the MR, allowed us to infer via ESR the symmetry of the Fermi surface of a compound. The effect of the magnetic polarons on the SFS rate of the conduction electrons clearly manifests itself in the  $H$  dependence of  $\Delta H$ .

Magnetic polarons are also invoked for other compounds displaying a large negative MR, e.g.,  $\text{EuO}$ , manganites, and manganese pyrochlores.<sup>16</sup> Here  $\text{EuO}$  is a semiconductor, requiring some doping, while for the manganese compounds the Mn ground state has orbital content (not an  $S$  state) and strongly couples to phonons (Jahn-Teller effect or lattice polarons). Hence, in manganites magnetic and lattice polarons play a role.  $\text{EuB}_6$ , on the other hand, is distinct from other systems, because it is a semimetal and  $\text{Eu}^{2+}$  is an  $S$  state, i.e., it has a carrier density that is low, yet sufficiently large for the formation of magnetic polarons without coupling to phonons. The nonmagnetic isoelectronic analog to  $\text{EuB}_6$  is  $\text{CaB}_6$ , which is a controversial high  $T_C$  FM with very small ordered magnetic moment.<sup>17</sup>

Single crystals of  $\text{EuB}_6$  (cubic, space group 221,  $Pm\bar{3}m$ , CsCl type) were grown as described in Ref. 17. The phase purity and orientation of the crystals were determined by powder and Laue x-ray diffraction, respectively. All ESR experiments were performed on a  $\sim 1 \times 1 \times 0.3$  mm<sup>3</sup> single crystal in a Bruker  $S$ ,  $X$ , and  $Q$  band spectrometer (4.1, 9.5, and 33.9 GHz) with resonators coupled to a helium gas flux  $T$ -controller system for  $4.2 \leq T \leq 300$  K.  $M(T, H)$  was measured for  $2 \leq T \leq 300$  K in a QD MPMS-5 superconducting quantum interference device-RSO direct current magnetometer.  $\rho(T, H, \theta)$  and  $c_p(T, H)$  were obtained in a QD PPMS-9 platform. For the  $\rho(T, H)$  measurements, the four contact method and a QD-horizontal rotator were used with  $H$  perpendicular to the current lines when  $H$  was rotated in the (100) plane, while if rotated in the (110) plane the angle

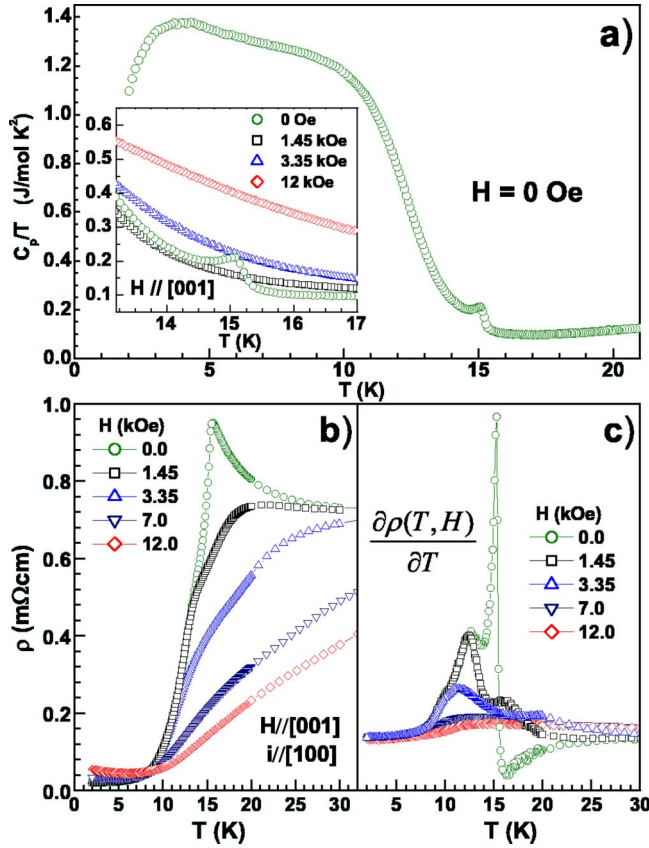


FIG. 1. (a)  $c_p(T)/T$  vs  $T$  for the  $\text{EuB}_6$  sample used in the ESR experiments. The inset shows the  $H$  dependence of  $c_p(T,H)/T$  around  $T_{c1}$  for  $H \parallel [001]$ ; (b)  $\rho(T,H)$  vs  $T$  for the same crystal for electric and magnetic fields along two perpendicular crystal axes; and (c)  $H$  evolution of the two transitions revealed by  $\partial\rho(T,H)/\partial T$ . The continuous lines are guides to the eyes.

between  $H$  and the current varies from  $90^\circ$  to  $45^\circ$ . The relaxation method was employed to measure  $c_p(T,H)$ .

Figures 1(a) and 1(b) show  $c_p(T,H)/T$  and  $\rho(T,H)$ , respectively. The entropy at high  $T$  saturates at  $R \ln(8)$  (not shown), which corresponds to the localized half-filled shell of  $\text{Eu}^{2+}$  ions. Our  $M(T,H)$  measurements are in agreement with those reported in Ref. 5. The high quality of our crystals is evidenced by the two magnetic transitions seen in  $\partial\rho(T,H)/\partial T$  [Fig. 1(c)] at  $T_{c1} \approx 15.3$  K and  $T_{c2} \approx 12.6$  K<sup>5-7</sup> and the resistivity ratio,  $\rho(298 \text{ K})/\rho(2 \text{ K}) \approx 100$ . The residual resistivity  $\rho(2 \text{ K}) \approx 17 \mu\Omega \text{ cm}$  shows that our  $\text{EuB}_6$  crystal has low carrier concentration ( $\sim 10^{20} \text{ cm}^{-3}$ ).<sup>4</sup>

All ESR spectra consist of a single unresolved resonance with a  $g$  value  $\sim 2.0$ , without *fine* and *hyperfine* structures, but with an *anisotropic*  $\Delta H$ . Figures 2(a) and 2(b) display the anisotropy of  $\Delta H$  for  $\text{EuB}_6$  at room- $T$  at three different microwave frequencies for  $H$  rotated in the (100) and (110) planes, respectively.  $\Delta H$  becomes narrower and more anisotropic as  $H$  increases. In all cases the angular variation of  $\Delta H$  follows the cubic symmetry of the crystal. The spectra for  $H$  along the [111] direction, where  $\Delta H$  is minimum, are shown in Fig. 2(c). The line shapes are clearly Dysonian<sup>18</sup> for all three frequencies, indicating that the  $\text{Eu}^{2+}$  ions in  $\text{EuB}_6$  experience a metallic environment and the  $A/B$  ratio is  $\approx 2.3$ ,

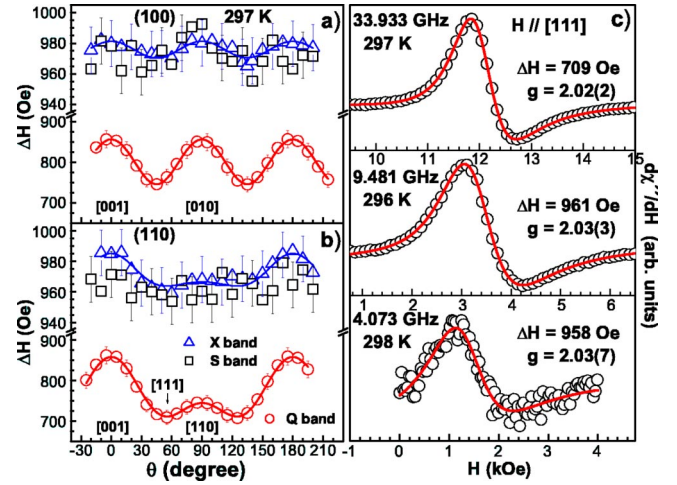


FIG. 2. (a) and (b) Room- $T$   $\Delta H$  anisotropies for  $\text{EuB}_6$  at three different microwave frequencies for  $H$  in the (100) and (110) planes, respectively. The solid lines are fittings using  $\Delta H^2(\theta, \phi) = A + Bf_4(\theta, \phi) + Cf_6(\theta, \phi)$  (see text); (c) the ESR spectra for  $H$  along the [111] direction in the (110) plane (minimum  $\Delta H$ ). The solid lines are fittings to a Dysonian line shape.

i.e., the skin depth is less than the size of the crystals.<sup>18</sup> From the *single metallic* resonance observed in the PM phase we conclude that there are no distinct resonances for the conduction and  $\text{Eu}^{2+}$ - $4f$  electrons. This is expected because the exchange coupling between the  $4f$  and conduction electrons is strong ( $J \approx 0.2 \text{ eV}$ ).<sup>6</sup>

The  $T$  dependence of  $\Delta H$  for  $T \geq 2T_c \approx 30$  K is shown in Fig. 3 for the three frequencies used and for  $H \parallel [001]$  and  $H \parallel [111]$ . Above  $T \approx 150$  K,  $\Delta H$  and its anisotropy are almost  $T$  independent for each frequency. This suggests that the spin-lattice relaxation either via the  $\text{Eu}^{2+}$ -conduction electron exchange interaction (Korringa mechanism) or via the spin-phonon (spin-orbit coupling) are both negligible. This is not unexpected, because  $\text{EuB}_6$  is a semimetal (low carrier density) and  $\text{Eu}^{2+}$  is an  $S$  state ion.

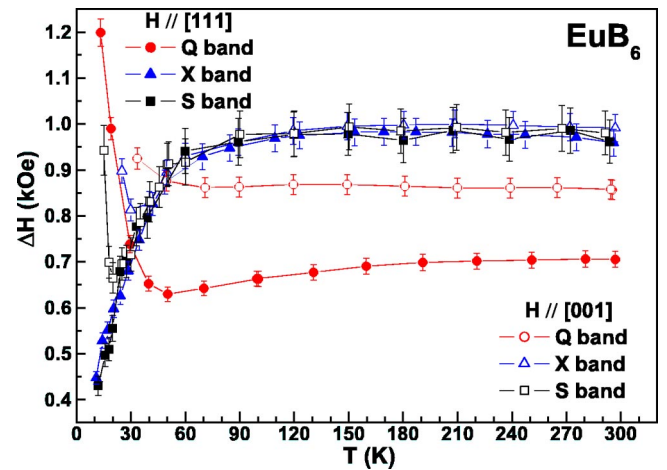


FIG. 3.  $T$  dependence of  $\Delta H$  for  $T \geq T_c$  with  $H \parallel [001]$  (open symbols) and  $H \parallel [111]$  (solid symbols) for the three ESR frequencies. The continuous lines are guides for the eyes.

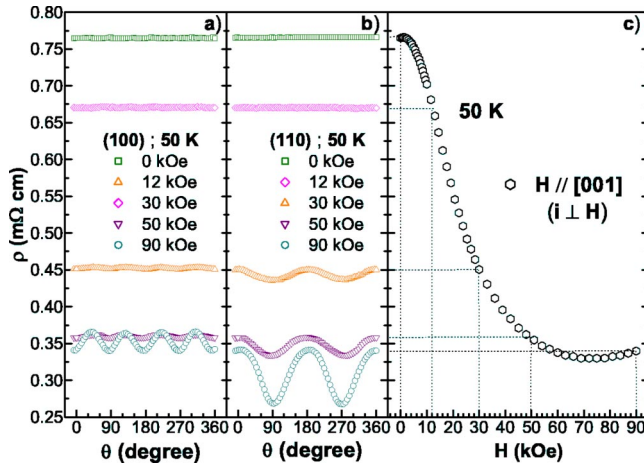


FIG. 4. (a) and (b) Anisotropy of the MR at  $T=50$  K for several  $H$  in the (100) and (110) planes, respectively, ( $\theta$ : angle between  $H$  and [001] axis; the current flows along the [100] direction); (c) MR,  $\rho(H)$ , at  $T=50$  K.

In contrast to the dilute Eu case,  $\text{Ca}_{1-x}\text{Eu}_x\text{B}_6$  ( $x \lesssim 0.0005$ ), no *fine* and *hyperfine* splittings were observed in our spectra.<sup>19</sup> Notice that the anisotropy of  $\Delta H$  cannot be attributed to an unresolved cubic crystal field of an  $S$ -state ion which predicts a minimum  $\Delta H$  at  $\theta=30^\circ$  from the [001] direction in the (110) plane.<sup>19</sup> In addition, as far as the linewidth is concerned, the ESR data of  $\text{Eu}_{1-x}\text{Ca}_x\text{B}_6$  ( $0 \leq x \leq 0.70$ ) give similar results to those presented in Fig. 2.<sup>20</sup> This allows us to exclude the dipolar interaction as the source of the line narrowing and anisotropy at high  $H$  in  $\text{EuB}_6$ .<sup>21</sup> The data in Figs. 1(a)–1(c) warrant the good quality of our crystals. The small amount of defects that may be present in the hexaborides ( $\leq 0.1\%$  of  $\text{B}_6$  vacancies),<sup>22</sup> are not sufficient to produce significant strain distribution in the samples. As shown in Figs. 2 and 3, unexpectedly,  $\Delta H$  is strongly reduced at higher  $H$  ( $Q$  band). All these results suggest that the resonance is homogeneous in the PM phase. The earlier arguments allow us to postulate that the main contribution to  $\Delta H$  arises from a SFS mechanism via the exchange coupling,  $J\mathbf{S}_{4f} \cdot \mathbf{s}_{cc}$ , between the spins of the  $\text{Eu}^{2+}4f$  electrons,  $\mathbf{S}_{4f}$ , and conduction electrons,  $\mathbf{s}_{cc}$ .

In Figs. 4(a) and 4(b) we present the anisotropy of the MR (current along the [100] direction) at  $T=50$  K and  $H=0, 1.2, 3, 5$ , and 9 T with  $H$  rotated in the (100) and (110) planes, respectively. The Fermi surface of  $\text{EuB}_6$  (small elliptical pockets at the  $X$  points) allows no open orbits that would complicate the analysis of the MR. For  $H \lesssim 3$  T, the MR is similar for both planes and has very small anisotropy. However, for  $H \geq 3$  T, the anisotropy of the resistivity increases as the field increases. The anisotropies are different for both planes, increase with  $H$ , and follow the cubic symmetry of the crystal. Similar anisotropies are obtained for  $T > 50$  K, although with a decreasing amplitude as  $T$  increases. At room- $T$  the amplitude is very small. The MR at 50 K and  $H \parallel [001]$  is presented in Fig. 4(c). Note that in the metallic FM phase at  $T=2$  K, we found similar anisotropic behavior for  $\rho(H, \theta)$ , but already for much lower  $H$ . The low- $T$  ( $T \lesssim 15$  K) and high- $H$  ( $H \geq 0.5$  T) MR is metallic, i.e.,

positive and proportional to  $H$ .<sup>2,4,6</sup> This contrasts the negative MR observed in the PM phase.

The  $T$  dependence of  $\rho$  in the PM phase has been attributed to the formation of magnetic polarons. In a magnetic polaron the spin of a conduction electron polarizes the  $\text{Eu}^{2+}$  spins in its neighborhood and drags the polarization cloud as it moves. Hall effect data showed that the number of carriers increases as  $T$  is lowered,<sup>11</sup> which is a consequence of the growth of the polarization clouds and the increase of magnetic correlations. The polarization clouds eventually percolate at  $T_{c1}$  and clear metallic behavior is obtained for  $T < T_{c1}$ . Long-range FM correlations are established below  $T_{c2}$  and  $\text{EuB}_6$  is driven into a metallic FM phase.<sup>8,9</sup> This increase of the magnetic correlations and the negative MR found in the PM phase, suggest the scenario of decreasing conduction electron SFS as  $T$  is lowered and  $H$  is increased.

We argue that the reported  $H$  and  $T$  dependence of  $\Delta H$  in  $\text{EuB}_6$  is a microscopic evidence for the earlier scenario. At high- $T$  ( $T \gtrsim 150$  K) as  $H$  increases the SFS is reduced giving rise to a reduction in  $\Delta H$  and to a *negative* MR (see Figs. 3 and 4). Also, the reduction of the  $\Delta H$  with  $T$  observed for  $T \lesssim 150$  K in the low- $H$  ( $S$  and  $X$  bands) ESR experiments (see Fig. 3) can be explained by the decrease in the SFS rate due to the increase in size of magnetic polarons. Note that the exchange  $J \gg T$  so that the spins of the electrons are always strongly correlated with the neighboring  $\text{Eu}^{2+}$  spins. Furthermore, the broadening of  $\Delta H$  found at low- $T$  ( $T \lesssim 50$  K) and higher  $H$  ( $Q$  band) (see Fig. 3) suggests that short-range magnetic correlations between polarons are present above  $T_{c1}$ . These short-range correlations may overcome the narrowing effect produced by the magnetic polarons by either generating a distribution of resonance fields (inhomogeneous broadening) or by relaxation into magnon-like excitations.

The anisotropy of  $\Delta H$  at room- $T$  [Figs. 2(a) and 2(b)] has cubic symmetry and increases at higher  $H$ . A similar result is observed for  $50 \text{ K} \leq T \leq 297 \text{ K}$ .  $\Delta H$  as a function of the angle between  $H$  and the [001] crystal axes for fixed  $T$  and  $H$  is given by  $\Delta H^2(\theta, \phi) = A + Bf_4(\theta, \phi) + Cf_6(\theta, \phi)$ . The parameters  $A$ ,  $B$ , and  $C$  are coefficients depending on  $H$  and  $T$ . The functions  $f_4(\theta, \phi)$  and  $f_6(\theta, \phi)$  are the linear combinations of spherical harmonics of fourth and sixth order having cubic symmetry.<sup>23</sup> The solid lines for the  $Q$ -band data are fittings to this equation giving  $A=595(2)$ ,  $B=17.6(5)$ , and  $C=0.1(1)\text{kOe}$ .

These results suggest that both, the high- $H$  resistivity and  $\Delta H$ , are sensitive to the  $\text{EuB}_6$  Fermi surface.<sup>24</sup> According to band structure calculations, de Haas-van Alphen and Shubnikov-de Haas measurements<sup>1-4</sup>  $\text{EuB}_6$  has *hole* and *electron* pockets at the  $X$  points of the Brillouin zone. The anisotropy of  $\Delta H$  is only weakly  $T$  dependent (see, e.g., the  $Q$ -band data in Fig. 3). This indicates that once the system behaves metallic at high fields  $\Delta H$  becomes sensitive to the Fermi surface. The higher sensitivity of  $\Delta H$  compared to the MR to reveal the symmetry of the Fermi surface at high- $T$  may be due to the fact that in  $\text{EuB}_6$  the main contribution to  $\Delta H$  comes from SFS with the conduction states,<sup>24</sup> while there are also other mechanisms contributing to the resistivity (e.g., electron-phonon scattering).

From the ESR and MR measurements in  $\text{EuB}_6$  reported here we conclude that  $\Delta H$  reveals the symmetry of the Fermi surface throughout the anisotropy in the SFS. Our results strongly suggest that the relaxation mechanism for the  $\text{Eu}^{2+}$  spins involves magnetic polarons. Small size polarons (a carrier correlating only the neighboring  $\text{Eu}^{2+}$  spins) probably exist even at room- $T$  (note  $J \gg T$ ). This observation was only possible due to the semimetallic character of  $\text{EuB}_6$ , i.e., the low carrier concentration, and the large exchange coupling  $J$ , giving rise to a homogeneous resonance with a linewidth dominated by SFS with the conduction states. The benefit of

low carrier concentration is twofold, *first*, it helps the formation of magnetic polarons clouds, thus reducing the SFS, and *second*, it suppresses the spin-lattice relaxation via the Korringa mechanism.<sup>25</sup>

The work at UNICAMP is supported by FAPESP and CNPq, and the work at the NHMFL by NSF Cooperative Agreement No. DMR-9527035 and the State of Florida. The support by NSF (Grant Nos. DMR-0102235 and DMR-0105431) and DOE (Grant No. DE-FG02-98ER45797) is also acknowledged.

- 
- <sup>1</sup>A. Hasegawa, and A. Yanase, *J. Phys. C* **12**, 5431 (1979).  
<sup>2</sup>S. Massidda, A. Continenza, T. M. de Pascale, and R. Monnier, *Z. Phys. B: Condens. Matter* **102**, 83 (1997).  
<sup>3</sup>R. G. Goodrich, N. Harrison, J. J. Vuillemin, A. Teklu, D. W. Hall, Z. Fisk, D. P. Young, and J. Sarrao, *Phys. Rev. B* **58**, 14 896 (1998).  
<sup>4</sup>M. C. Aronson, J. L. Sarrao, Z. Fisk, M. Whitton, and B. L. Brandt, *Phys. Rev. B* **59**, 4720 (1999).  
<sup>5</sup>S. Süllow, I. Prasad, M. C. Aronson, J. L. Sarrao, Z. Fisk, D. Hristova, A. H. Lacerda, M. E. Hundley, A. Vigliante, and D. Gibbs, *Phys. Rev. B* **57**, 5860 (1998).  
<sup>6</sup>S. Süllow, I. Prasad, M. C. Aronson, S. Bogdanovich, J. L. Sarrao, and Z. Fisk, *Phys. Rev. B* **62**, 11 626 (2000).  
<sup>7</sup>L. Degiorgi, E. Felder, H. R. Ott, J. L. Sarrao, and Z. Fisk, *Phys. Rev. Lett.* **79**, 5134 (1997).  
<sup>8</sup>P. Nyhus, S. Yoon, M. Kauffman, S. L. Cooper, Z. Fisk, and J. L. Sarrao, *Phys. Rev. B* **56**, 2717 (1997).  
<sup>9</sup>C. S. Snow, S. L. Cooper, D. P. Young, and Z. Fisk, *Phys. Rev. B* **64**, 174412 (2001).  
<sup>10</sup>S. Broderick, B. Ruzicka, L. Degiorgi, H. R. Ott, J. L. Sarrao, and Z. Fisk, *Phys. Rev. B* **65**, 121102 (2002).  
<sup>11</sup>S. Paschen, D. Pushin, M. Schlatter, P. Vontanthan, H. R. Ott, D. P. Young, and Z. Fisk, *Phys. Rev. B* **61**, 4174 (2000).  
<sup>12</sup>Z. Fisk, D. C. Johnston, B. Cornut, S. von Molnar, S. Oseroff, and R. Calvo, *J. Appl. Phys.* **50**, 1911 (1979).  
<sup>13</sup>W. Henggeler, H. R. Ott, D. P. Young, and Z. Fisk, *Solid State Commun.* **108**, 929 (1998).  
<sup>14</sup>W. S. Glaunsinger, *Phys. Status Solidi B* **74**, 443 (1976).  
<sup>15</sup>S. Oseroff, R. Calvo, J. Stankiewicz, Z. Fisk, and J. D. Johnston, *Phys. Status Solidi B* **94**, K133 (1979).  
<sup>16</sup>M. A. Subramanian, B. H. Toby, J. W. Marshall, A. P. Ramirez, A. W. Sleight, and G. W. Kwei, *Science* **273**, 81 (1996); A. P. Ramirez, *J. Phys.: Condens. Matter* **9**, 8171 (1997); A. Asamitsu, Y. Moritomo, Y. Tomioka, T. Arima, and Y. Tokura, *Nature (London)* **373**, 407 (1995); A. J. Millis, *ibid.* **392**, 147 (1998); A. J. Millis, *ibid.* **74**, 5144 (1995).  
<sup>17</sup>D. P. Young, D. Hall, M. E. Torelli, Z. Fisk, J. L. Sarrao, J. D. Thompson, H.-R. Ott, S. B. Oseroff, R. G. Goodrich, and R. Zysler, *Nature (London)* **397**, 412 (1999).  
<sup>18</sup>G. Feher and A. F. Kip, *Phys. Rev.* **98**, 337 (1955); F. J. Dyson, *ibid.* **98**, 349 (1955); G. E. Pake and E. M. Purcell, *ibid.* **74**, 1184 (1948).  
<sup>19</sup>R. R. Urbano, C. Rettori, G. E. Barberis, M. Torelli, A. Bianchi, Z. Fisk, P. G. Pagliuso, A. Malinowski, M. F. Hundley, J. L. Sarrao, and S. B. Oseroff, *Phys. Rev. B* **65**, 180407 (2002).  
<sup>20</sup>R. R. Urbano, P. G. Pagliuso, C. Rettori, P. Schlottmann, J. L. Sarrao, A. Bianchi, S. Nakatsuji, Z. Fisk, and S. B. Oseroff (unpublished).  
<sup>21</sup>G. Sperlich and K. Jansen, *Solid State Commun.* **15**, 1105 (1974).  
<sup>22</sup>M. A. Noack and J. D. Verhoeven, *J. Cryst. Growth* **49**, 595 (1980).  
<sup>23</sup>S. B. Oseroff and R. Calvo, *Phys. Rev. B* **18**, 3041 (1978).  
<sup>24</sup>D. Davidov, K. Maki, R. Orbach, C. Rettori, and E. P. Chock, *Solid State Commun.* **12**, 621 (1973).  
<sup>25</sup>C. Rettori, D. Davidov, R. Orbach, E. P. Chock, and B. Ricks, *Phys. Rev. B* **7**, 1 (1973).